Nonequilibrium stationary state of a harmonic crystal with alternating masses

Venkateshan Kannan,[1] Abhishek Dhar,[2] and J. L. Lebowitz[1]

[1]*Departments of Mathematics and Physics, Rutgers University, Piscataway, New Jersey 08854, USA*

[2]*Raman Research Institute, Bangalore 560080, India*

We analyze the nonequilibrium steady states (NESS) of a one-dimensional harmonic chain of N atoms with alternating masses connected to heat reservoirs at unequal temperatures. We find that the temperature profile defined through the local kinetic energy $T(j) \equiv \langle p_j^2 \rangle / m_j$ oscillates with period two in the bulk of the system. Depending on boundary conditions, either the heavier or the lighter particles in the bulk are hotter. We obtain explicit integral expressions for the bulk temperature profile and steady state current in the limit $N \rightarrow \infty$. These depend on whether N is odd or even. We also study similar temperature oscillations in the NESS of systems with noise in the dynamics. These die out as $N \rightarrow \infty$.

I. INTRODUCTION

The study of nonequilibrium steady states (NESS) of macroscopic systems in contact with heat baths at different temperatures has a long history [1–3]. There are no known analytic solutions for interacting Hamiltonian systems, except for harmonic crystals. When the atoms in the crystal all have the same mass, this NESS can be obtained explicitly [4,5]. It gives a uniform "temperature," i.e., $\langle p_j^2 \rangle / m$, in the bulk of the system. It also gives heat currents that are independent of the size of the system corresponding to the fact that phonons can travel freely through the crystal. This behavior of the heat current is also true for harmonic systems with periodic arrangement of masses [6,7]. It was therefore surprising when numerical simulations of the NESS showed that the bulk temperature profile of a chain with alternating masses oscillates between two values and that these oscillations did not seem to decay upon increasing the system size [1].

Here we present analytical solutions for the temperature profile and current in the alternate-mass chain connected to Langevin type heat baths, which prove that the oscillations persist in the $N \rightarrow \infty$ limit. Only for very special choices of parameter values, can the oscillations be made to vanish. Surprisingly, the values of the oscillating temperature and of the current depend on whether N is even or odd even in the asymptotic system size limit. An oscillating temperature profile in a thermodynamically large system is surprising when we think from the standard viewpoint of heat flow occurring from hot to cold regions. However this expectation will be true only in systems exhibiting local thermal equilibrium where one can define a meaningful thermodynamic local temperature. This is the case for a system with normal diffusive heat transport, though a microscopic derivation of the conditions when this is achieved is in general difficult [2]. In the study of systems in NESS it is natural to define a local "temperature" from the mean local kinetic energy and this is what we do here—the absence of local equilibrium in the harmonic chain allows for the "temperature" profile to show the unexpected oscillatory feature.

We note here that the study of one-dimensional models with alternating masses has a long history [8–16]. The alternating mass harmonic chain which is the focus of the present article was first studied in [6]. An exact explicit expression for the current in the case of a chain with an even number of sites was given in [7] and then in [14]. It was noted in [14] that the current is proportional to $(\frac{m}{M})$, the ratio of the light to heavy masses when $\frac{m}{M} \rightarrow 0$. This would make the current smaller in the alternating mass chain than in a monoatomic chain with only particles of mass m.

Temperature oscillations have earlier been observed in the steady state of the alternate mass hard particle gas [15] and in the Fermi-Pasta-Ulam chain [16] but in these cases the oscillations decay with system size. The case of temperature oscillations persisting for infinite system sizes is thus special to harmonic systems where heat is transmitted by noninteracting phonons. It is expected that the introduction of phonon-phonon interactions will in general make things different. Here we investigate this issue by considering alternate-mass harmonic chains where the dynamics is stochastically perturbed by noise which either conserves both energy and momentum or conserves only energy. Finally, to consider the effect of dimensionality, we present results from simulations of two-dimensional strips of alternate mass harmonic systems.

The plan of the paper is as follows. In Sec. II we define the precise model and present some of the numerical results for small finite systems. In Sec. III we present the analytic and numerical results in the limit $N \rightarrow \infty$. In Sec. IV we present simulation results on temperature profiles in harmonic chains with noisy dynamics. In Sec. V we summarize our results and give a physical explanation of the results. The details of our analytical calculations are given in the Appendix.

II. MODEL AND NUMERICAL RESULTS FOR SMALL SYSTEM SIZES

We consider a one-dimensional chain of N particles labeled $i = 1, \ldots, N$ that are placed in an external harmonic potential (with spring constant k_o) and which are interacting with each other through a nearest neighbor harmonic potential (with spring constant k). Let the vectors $q = (q_1, q_2, \ldots, q_N)$ and $p = (p_1, p_2, \ldots, p_N)$ denote respectively the displacement and momenta of the N particles of the chain. The Hamiltonian for

the 1D chain we consider is given by

$$H = \frac{1}{2}\sum_{i=1}^{i=N} p_i^2/2m_i + \frac{1}{2}\sum_{i=1}^{N+1} k(q_i - q_{i-1})^2 + \frac{1}{2}\sum_{i=1}^{N} k_o q_i^2 \quad (1)$$

$$= \frac{1}{2} p \cdot \mathbf{M}^{-1} \cdot p + \frac{1}{2} q \cdot \mathbf{\Phi} \cdot q, \quad (2)$$

with $q_0 = q_{N+1} = 0$, and in the second line we have used a compact notation with $\mathbf{M}$ defining the mass matrix and $\mathbf{\Phi}$ the force matrix. The ends of the chain are coupled to Langevin reservoirs at temperatures T_L and T_R. The equations of motion of the system are given by

$$m_i \ddot{q}_i = -\sum_{j=1,N} \Phi_{i,j} q_j + \delta_{i,1}[-\gamma_L \dot{q}_1 + (2\gamma_L T_L)^{1/2}\eta_L]$$

$$+ \delta_{i,N}[-\gamma_R \dot{q}_N + (2\gamma_R T_R)^{1/2}\eta_R], \quad (3)$$

for $i = 1, 2, \ldots, N$, where η_L, η_R are Gaussian white noises chosen from distributions with averages $\langle \eta_L(t)\rangle = \langle \eta_R(t)\rangle = 0$ and correlations $\langle \eta_L(t)\eta_L(t')\rangle = \langle \eta_R(t)\eta_R(t')\rangle = \delta(t - t')$, and γ_L, γ_R are dissipation constants. (Note that the derivation in [6] uses a different convention for the reservoir coupling. The dissipative forces on the end particles were there taken to be $-\lambda_1 p_1$ and $-\lambda_N p_N$ and so their coupling constants are related to ours as $\lambda_1 m_1 = \gamma_L, \lambda_N m_N = \gamma_R$.) We will be interested in the case where the masses m_i alternate between two values m_a and m_b on successive sites.

Corresponding to the Langevin equations in Eq. (3) it is straightforward to write the Fokker-Planck equation to describe the evolution of the phase space distribution $\mu(x,t), x = (q_1, \ldots, q_N, p_1, \ldots, p_N)$. Following standard methods [18] it can be shown that the Fokker-Planck equation is given by

$$\frac{\partial\mu}{\partial t} + \sum_{i=1}^{N}\left[\frac{p_i}{m_i}\frac{\partial\mu}{\partial q_i} - \sum_{j=1}^{N}\Phi_{i,j}q_j\frac{\partial\mu}{\partial p_i}\right]$$

$$= \sum_{i=1,N}\frac{\gamma_i}{m_i}\frac{\partial}{\partial p_i}\left[p_i\mu + T_i m_i\frac{\partial\mu}{\partial p_i}\right], \quad (4)$$

where the right-hand side of Eq. (4) describes the interaction of the end particles with the heat baths and $T_{1,N} = T_{L,R}$ and $\gamma_{1,N} = \gamma_{L,R}$. Let us define the $2N \times 2N$ matrix

$$\mathbf{a} = \begin{pmatrix} \mathbf{0} & -\mathbf{M}^{-1} \\ \mathbf{\Phi} & \mathbf{M}^{-1}\mathbf{\Gamma} \end{pmatrix}, \quad (5)$$

where $\mathbf{\Gamma}$ is a $N \times N$ diagonal matrix with $\Gamma_{ij} = \gamma_i\delta_{ij}(\delta_{i1} + \delta_{iN})$. We also define the $2N \times 2N$ matrix $\mathbf{d}$ with elements $d_{ij} = 2\gamma\delta_{ij}(T_L\delta_{i,N+1} + T_R\delta_{i,2N})$. It is known that the steady state distribution is Gaussian [4] and given by

$$\mu_s = (2\pi)^{-N}\text{Det}[\mathbf{b}]^{-1/2}\exp\left(-\frac{1}{2}\sum_{i,j=1}^{2N}b_{ij}^{-1}x_i x_j\right),$$

where the covariance matrix $\mathbf{b}$ with elements $b_{ij} = \langle x_i x_j\rangle$ satisfies

$$\mathbf{a}\cdot\mathbf{b} + \mathbf{b}\cdot\mathbf{a}^\dagger = \mathbf{d}. \quad (6)$$

The solution of the linear equations, Eq. (6), gives us all the correlations b_{ij} and hence the temperature profile $T_i = \langle p_i^2\rangle/m_i = b_{N+i,N+1}/m_i$, and the current, $J = k\langle(q_{i+1} -$
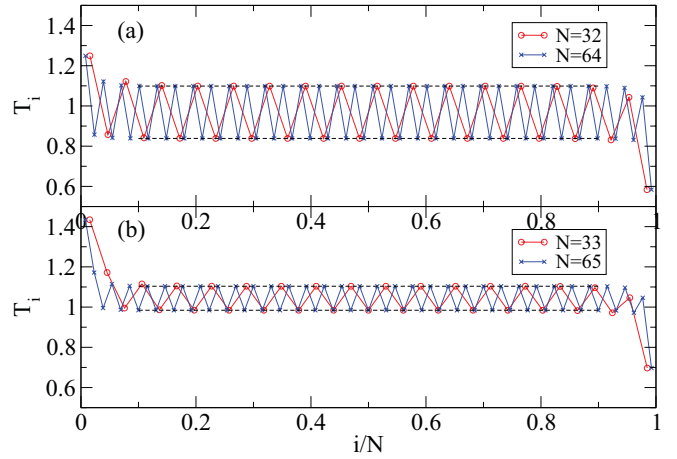

FIG. 1. (Color online) Temperature profiles for (a) system with even number of sites $N = 32, 64$ and with $\gamma_L = \gamma_R = 1.0$ and (b) system with odd number of sites $N = 33, 65$ and with $\gamma_L = 1.5, \gamma_R = 0.5$. Other parameters were set to $m_a = 0.75, m_b = 0.25, k = 1, T_L = 1.5, T_R = 0.5$. The mass of the first particle is always taken to be m_a. Note that in (a), the heavier particles are hotter, while in (b), the lighter particles are hotter. The horizontal dashed lines indicate the analytic predictions for $N \to \infty$, from Eqs. (11), (12).

$q_i)p_i/m_i\rangle = k(b_{i+1,N+i} - b_{i,N+i})/m_i$. In the equal mass case the covariance matrix for N sites can be obtained in a fairly explicit form [4]. This seems to be difficult for the alternate mass case. However the matrix equations can be solved numerically for small system sizes and we can obtain accurate results for the temperature profile and current for these system sizes. In Fig. 1 we show typical temperature profiles for alternate mass chains with even and odd number of sites for particular choices of parameter values and N. We see oscillations in the temperatures of the particles in the bulk in both the even and odd cases, and the amplitude of the oscillations does not seem to change with system size. In the next section, we will obtain expressions for the current and the bulk temperatures and show that the temperature oscillations persist in the $N \to \infty$ limit.

III. ANALYTICAL AND NUMERICAL RESULTS IN $N \to \infty$ LIMIT

To obtain analytic results in the limit $N \to \infty$ we follow [6] and express the covariances in terms of integrals over frequencies. The integrands involve elements of the following Green's function:

$$\mathbf{G}^+ = [-\mathbf{M}\omega^2 + \mathbf{\Phi} - i\omega\mathbf{\Gamma}]^{-1}. \quad (7)$$

Here we are interested in the temperature and current and these are given by [6,17]

$$T_i = \frac{1}{\pi}m_i\left[\gamma_L T_L\int_{-\infty}^{\infty}d\omega\,\omega^2|\mathbf{G}_{i1}^+(\omega)|^2\right.$$

$$\left. + \gamma_R T_R\int_{-\infty}^{\infty}d\omega\,\omega^2|\mathbf{G}_{iN}^+(\omega)|^2\right], i = 1, 2, \ldots, N,$$

$$J = \frac{\gamma_L\gamma_R(T_L - T_R)}{\pi}\int_{-\infty}^{\infty}d\omega\,\omega^2|\mathbf{G}_{1,N}^+(\omega)|^2. \quad (8)$$

We rewrite the above expressions in the form

$$T_i = I_i T_L + \hat{I}_i T_R,$$
$$J = \frac{\gamma_R}{m_N}(T_L - T_R)I_N,$$

where the

$$I_i = \frac{m_i \gamma_L}{\pi} \int_{-\infty}^{\infty} d\omega \, \omega^2 |\mathbf{G}_{i1}^{+}(\omega)|^2,$$
$$\hat{I}_i = \frac{m_i \gamma_R}{\pi} \int_{-\infty}^{\infty} d\omega \, \omega^2 |\mathbf{G}_{iN}^{+}(\omega)|^2 \tag{9}$$

are independent of the temperatures T_L and T_R. Now we note that for the equilibrium case $T_L = T_R$, we must have the same temperature at all sites, i.e., $T_i = T$, and hence deduce the equality $I_i + \hat{I}_i = 1$. Using this fact and defining $T_L = T + \Delta T/2$, $T_R = T - \Delta T/2$, we can rewrite the equation for the temperature profile in the form

$$T_i = T + (I_i - 1/2)\Delta T = T_R + I_i \Delta T. \tag{10}$$

We thus only need to evaluate the integral I_i, in the limit $N \to \infty$.

So far our treatment has been quite general. We now focus on the alternate mass case. We define the first mass to be $m_1 = m_a$ and the next to be m_b and so on. Thus odd sites have $m_i = m_a$ and even sites, $m_i = m_b$. For simplicity we only consider the unpinned case $k_o = 0$. It is straightforward to extend the calculations to the case $k_o \neq 0$. Without loss of generality we can choose time and energy scales so that $k = 1$ and $m_a + m_b = 1$. We give the details of the calculation in the Appendix. The main result is that I_i can be written as a sum of two parts, one coming from the acoustic modes of the system and one from the optical modes. We note that the mode frequencies for the acoustic and optical bands are respectively given by $\omega_-^2 = (1/m_a m_b)[1 - \phi(q)]$, $\omega_+^2 = (1/m_a m_b)[1 + \phi(q)]$, where $\phi(q) = [1 - 2m_a m_b(1 - \cos q)]^{1/2}$, $0 \leqslant q \leqslant \pi$. The various expressions depend on whether N is even or odd and for these two cases corresponding to superscript E, O respectively, we get the following:

Case (1) $N = 2L$, $L \to \infty$:

$$T_o^E = T + \Delta T \left[\int_0^\pi dq \frac{\gamma_L m_a}{2\pi\phi(q)} \frac{(m_b \omega_+^2 - 2)^2 + 4\gamma_R^2 \omega_+^2 \cos^2(q/2)}{|2(\gamma_L + \gamma_R) - (m_a \gamma_R + m_b \gamma_L)\omega_+^2|(1 + \gamma_L \gamma_R \omega_+^2)} \right.$$
$$\left. + \int_0^\pi dq \frac{\gamma_L m_a}{2\pi\phi(q)} \frac{(m_b \omega_-^2 - 2)^2 + 4\gamma_R^2 \omega_-^2 \cos^2(q/2)}{|2(\gamma_L + \gamma_R) - (m_a \gamma_R + m_b \gamma_L)\omega_-^2|(1 + \gamma_L \gamma_R \omega_-^2)} - \frac{1}{2} \right],$$

$$T_e^E = T + \Delta T \left[\int_0^\pi dq \frac{\gamma_L m_b}{2\pi\phi(q)} \frac{4\cos^2(q/2) + \gamma_R^2 \omega_+^2(m_a \omega_+^2 - 2)^2}{|2(\gamma_L + \gamma_R) - (m_a \gamma_R + m_b \gamma_L)\omega_+^2|(1 + \gamma_L \gamma_R \omega_+^2)} \right.$$
$$\left. + \int_0^\pi dq \frac{\gamma_L m_b}{2\pi\phi(q)} \frac{4\cos^2(q/2) + \gamma_R^2 \omega_-^2(m_a \omega_-^2 - 2)^2}{|2(\gamma_L + \gamma_R) - (m_a \gamma_R + m_b \gamma_L)\omega_-^2|(1 + \gamma_L \gamma_R \omega_-^2)} - \frac{1}{2} \right],$$

$$J^E = \Delta T \left[\int_0^\pi dq \frac{\gamma_L \gamma_R}{\pi\phi(q)} \frac{\sin^2 q}{|2(\gamma_L + \gamma_R) - (m_a \gamma_R + m_b \gamma_L)\omega_+^2|(1 + \gamma_L \gamma_R \omega_+^2)} \right.$$
$$\left. + \int_0^\pi dq \frac{\gamma_L \gamma_R}{\pi\phi(q)} \frac{\sin^2 q}{|2(\gamma_L + \gamma_R) - (m_a \gamma_R + m_b \gamma_L)\omega_-^2|(1 + \gamma_L \gamma_R \omega_-^2)} \right], \tag{11}$$

where the subscript o refers to odd sites and e to even sites.
Case (2) $N = 2L + 1$, $L \to \infty$:

$$T_o^O = T + \Delta T \left[\int_0^\pi dq \frac{\gamma_L m_a}{2(\gamma_L + \gamma_R)\pi\phi(q)} \frac{4\cos^2(q/2) + \gamma_R^2 \omega_+^2(m_b \omega_+^2 - 2)^2}{|(m_a \omega_+^2 - 2) + \gamma_L \gamma_R \omega_+^2(m_b \omega_+^2 - 2)|} \right.$$
$$\left. + \int_0^\pi dq \frac{\gamma_L m_a}{2(\gamma_L + \gamma_R)\pi\phi(q)} \frac{4\cos^2(q/2) + \gamma_R^2 \omega_-^2(m_b \omega_-^2 - 2)^2}{|(m_a \omega_-^2 - 2) + \gamma_L \gamma_R \omega_-^2(m_b \omega_-^2 - 2)|} - \frac{1}{2} \right],$$

$$T_e^O = T + \Delta T \left[\int_0^\pi dq \frac{\gamma_L m_b}{2(\gamma_L + \gamma_R)\pi\phi(q)} \frac{(m_a \omega_+^2 - 2)^2 + 4\gamma_R^2 \omega_+^2 \cos^2(q/2)}{|(m_a \omega_+^2 - 2) + \gamma_L \gamma_R \omega_+^2(m_b \omega_+^2 - 2)|} \right.$$
$$\left. + \int_0^\pi dq \frac{\gamma_L m_b}{2(\gamma_L + \gamma_R)\pi\phi(q)} \frac{(m_a \omega_-^2 - 2)^2 + 4\gamma_R^2 \omega_-^2 \cos^2(q/2)}{|(m_a \omega_-^2 - 2) + \gamma_L \gamma_R \omega_-^2(m_b \omega_-^2 - 2)|} - \frac{1}{2} \right],$$

$$J^O = \Delta T \left[\int_0^\pi dq \frac{\gamma_L \gamma_R}{(\gamma_L + \gamma_R)\pi\phi(q)} \frac{\sin^2 q}{|(m_a \omega_+^2 - 2) + \gamma_L \gamma_R \omega_+^2(m_b \omega_+^2 - 2)|} \right.$$
$$\left. + \int_0^\pi dq \frac{\gamma_L \gamma_R}{(\gamma_L + \gamma_R)\pi\phi(q)} \frac{\sin^2 q}{|(m_a \omega_-^2 - 2) + \gamma_L \gamma_R \omega_-^2(m_b \omega_-^2 - 2)|} \right]. \tag{12}$$
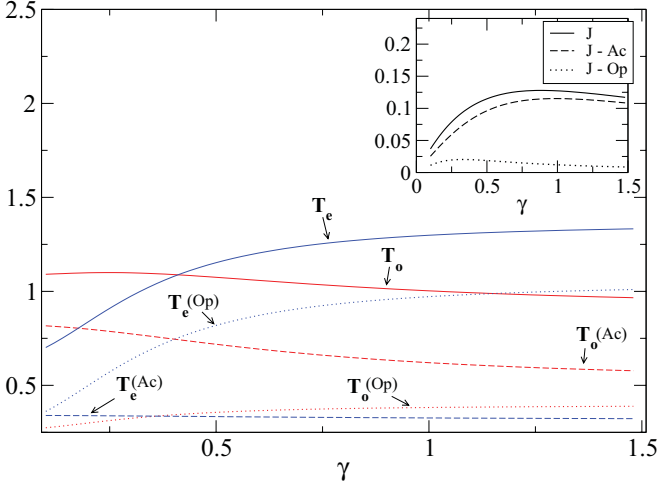
FIG. 2. (Color online) Temperatures at odd and even sites for a chain with even number of particles, plotted as a function of $\gamma = \gamma_L = \gamma_R$, $m_a = 0.75, m_b = 0.25, k = 1, T_L = 1.5, T_R = 0.5$. We also plot separately the contributions of the acoustic and optical modes to the temperature at any site. The inset shows J and also the contributions of the acoustic and optical modes.

FIG. 3. (Color online) Temperatures at odd and even sites for a chain with odd number of particles, plotted as a function of γ_R with $\gamma_L = 1$, $m_a = 0.75, m_b = 0.25, k = 1, T_L = 1.5, T_R = 0.5$. We also plot separately the contributions of the acoustic and optical modes to the temperature at any site. The inset shows the variation of heat current with γ_R and also the contributions of the acoustic and optical modes.

We now present some numerical data for the two cases of even N and odd N for various parameter sets. When $\gamma_L = \gamma_R$, the above integrals can be carried out exactly; see Eqs. (A13)–(A17). In other cases, we evaluated the integrals numerically (using MATHEMATICA).

Case (1) We consider chains with even N and set $\gamma_L = \gamma_R = \gamma$. In Fig. 2 we plot the temperatures on the odd (T_o^E) and even (T_e^E) sites, and also the current (J^E in inset) as a function of the parameter γ. We also separately plot the contributions of the acoustic and optical modes to the temperatures and current. We note the following features:

(i) Depending on the value of γ, either the heavier particles (those on odd sites) or the lighter ones are hotter. At $\gamma \approx 0.41$, the temperatures at the odd and even sites are equal.

(ii) The temperature of the heavier particles gets its main contribution from the acoustic modes while that of the lighter particles comes mostly from the optical modes. The heat current is mostly carried by the acoustic modes.

Case (2) We consider chains with odd N. In this case, $\gamma_L = \gamma_R$ becomes a very special case: The masses of the end particles being equal, this condition implies symmetry between the left and right reservoirs, and this leads to a uniform bulk temperature equal to $(T_L + T_R)/2$. The more typical situation is when the two couplings are different and we consider this by setting $\gamma_L = 1$ and changing γ_R. In Fig. 3 we plot the temperatures on the odd (T_o^O) and even (T_e^O) sites, and also the current (J^O in inset) as a function of the parameter γ_R. We also separately plot the contributions of the acoustic and optical modes to the temperatures and current. We note the following features:

(i) Depending on the value of γ_R, either the heavier particles (those on odd sites) or the lighter ones are hotter. At a special value of $\gamma_R = \gamma_L$, the temperatures at the odd and even sites are the same. They are both equal to the mean temperature $T = 1$.
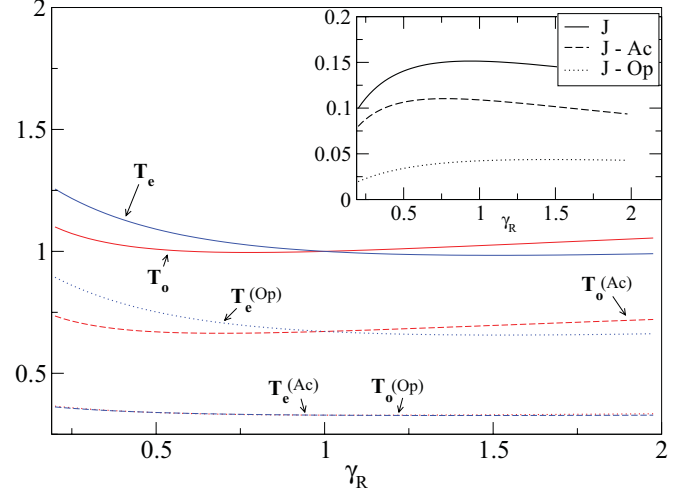
(ii) As for the even N case, here also we see that the temperature of the heavier particles gets it main contribution from the acoustic modes while that of the lighter particles comes mostly from the optical modes. The heat current is again mostly carried by the acoustic modes.

IV. SIMULATION RESULTS ON THE EFFECT OF NOISE IN THE DYNAMICS

As discussed in the introduction, temperature oscillations have been observed in anharmonic chains, where however the oscillations decay with system size. This is expected since anharmonicity leads to interactions between phonons which helps to establish local thermal equilibrium. A simple model which incorporates phonon-phonon interactions was introduced in [19,20] where the deterministic dynamics of the harmonic chain is stochastically perturbed. Here we have carried out simulations with this noisy dynamics and looked at its effect on the temperature profiles of the alternating mass chain. There are two cases to consider:

(a) *Momentum-conserving noise.* Here, in addition to the Hamiltonian dynamics without pinning, one introduces random exchange of momentum between nearest neighbor particles, which occurs with a rate λ. This conserves both momentum and energy. In Figs. 4 and 5 we show the effect of momentum-conserving noise on the temperature profiles for chains of even and odd number of particles. In the even N case we see that, on introducing noise, the size of the oscillations has decreased and the phase of the oscillation on the left half has changed sign. For the odd case, the choice of parameters ($\gamma_L = \gamma_R = 1$) corresponds to a case with no oscillations when $\lambda = 0$. On introducing noise, $\lambda > 0$, one gets oscillations very similar to the even N case. We also see that the oscillation amplitude becomes smaller upon increasing system size, for both even and odd N cases.
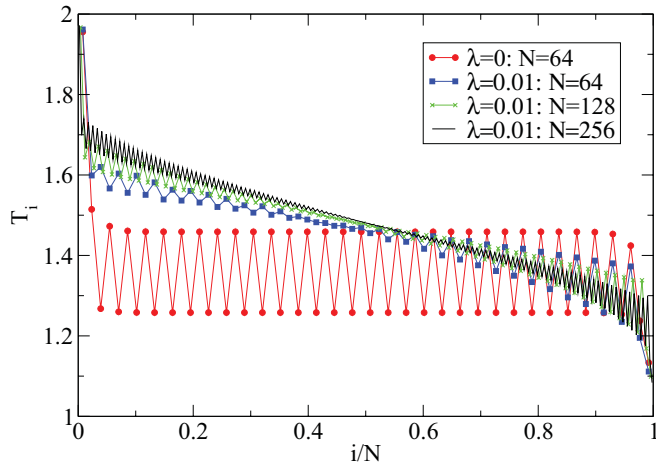
FIG. 4. (Color online) Temperature profiles with energy- and momentum-conserving noisy dynamics for a harmonic chain with even number of particles. Other parameters were taken to be $m_a = 0.5$, $m_b = 1.5$, $\gamma_L = \gamma_R = 1.0$ and $T_L = 2.0, T_R = 1.0$.
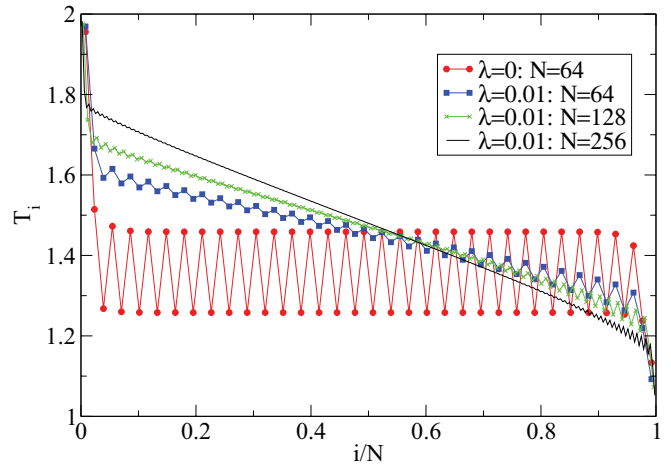

FIG. 6. (Color online) Temperature profiles with only energy-conserving noisy dynamics for a harmonic chain with even number of particles. Other parameters were taken to be $m_a = 0.5$, $m_b = 1.5$, $\gamma_L = \gamma_R = 1.0$ and $T_L = 2.0, T_R = 1.0$.

Thus we see that the temperature profile in this system with energy-momentum-conserving noisy dynamics shows the following qualitative features: (i) The oscillations decay as we go into the bulk. (ii) There is a phase shift in the sign of the oscillation amplitude as one crosses the center of the chain. The lighter particles at the hot end are always hotter than the heavier particles. At the cold end, the heavier particles are hotter. Thus this is *qualitatively* different from the harmonic case. (iii) For large N, the temperature profile is not sensitive to whether N is even or odd. These same features have also been observed earlier for the alternate mass FPU chain [16] which had a quartic interparticle interaction potential (in addition to the harmonic one). The FPU system has momentum conservation and does not satisfy Fourier's law as is also the case for the system with noisy dynamics.

(b) *Momentum-nonconserving case.* When the noise only conserves energy but not momentum, as can be obtained by

randomly reversing the velocity of the ith particle at rate λ, then, as is seen in [21,22], the NESS for $N \to \infty$ corresponds to a local equilibrium state. This ensures that the T_i in the bulk is the same for i odd or even independently of whether N is even or odd. In Figs. 6 and 7, we show the effect of addition of velocity flipping dynamics on the temperature profile for harmonic chains with odd and even number of particles. We observe that for the even case, the oscillations in the temperature decreases considerably upon introducing the noise, and this reduction is greater when N is larger. For the odd case however, for small systems, introduction of noise produces small oscillations in the temperature profile, but these oscillations eventually decrease as the system size is increased. For both even and odd total number of particles, the decay of the oscillation amplitude with system size is faster than for the momentum-conserving case and we quickly get a linear temperature profile in the bulk of the system.
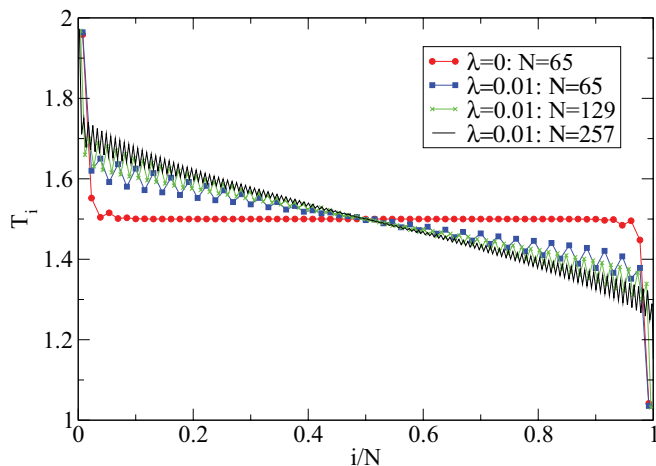

FIG. 5. (Color online) Temperature profiles with energy- and momentum-conserving noisy dynamics for a harmonic chain with an odd number of particles. Other parameters were taken to be $m_a = 0.5$, $m_b = 1.5$, $\gamma_L = \gamma_R = 1.0$ and $T_L = 2.0, T_R = 1.0$.
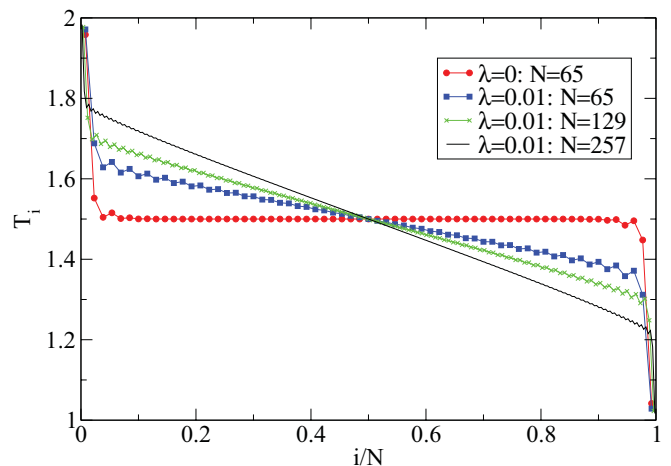

FIG. 7. (Color online) Temperature profiles with only energy-conserving noisy dynamics for a harmonic chain with an odd number of particles. Other parameters were taken to be $m_a = 0.5$, $m_b = 1.5$, $\gamma_L = \gamma_R = 1.0$ and $T_L = 2.0, T_R = 1.0$.

V. DISCUSSION

In this paper we obtained exact expressions for the temperature profile and the heat current in the alternate mass chain connected to heat baths at different temperatures in the limit of infinite system size. This proves rigorously that the temperature oscillations of successive particles in the bulk persist even in the thermodynamic limit.

We provided an understanding of these oscillations by noting that in any given normal mode, the mean kinetic energy of a particle depends on its mass. In an acoustic mode, the heavier particles have higher mean kinetic energy than the lighter ones, while in an optical mode, the lighter particles have higher kinetic energy. Upon connecting the chain to heat reservoirs each of the modes are excited to different degrees, depending on the parameters. The kinetic energy of a particle gets contributions from all the modes, both acoustic and optical, and the net result depends on the distribution of energy in the different modes. If both the baths have the same temperature, we have an equilibrium steady state in which each mode has the same average energy (equipartition). In this case the temperatures at all sites are equal. The same is true locally when the system is in local equilibrium.

The situation is different in the nonequilibrium case where we do not have local equilibrium and there is no equipartition of energy between the different modes. We then expect generically that the mean kinetic energy (temperatures) obtained by adding the contributions of all modes will depend

on the mass of the particle. It is therefore not so surprising that we get different kinetic energies for the different masses. From the above explanation we expect that temperature oscillations should also occur in higher dimensional periodic harmonic systems. Simulation results for two-dimensional strips (see Fig. 8) suggest that this is the case, but more extensive studies are necessary to establish the role of dimensionality.

As already noted there will be no oscillations in the bulk if the NESS is in local thermal equilibrium. To achieve this one introduces interactions between the phonons. Interactions between phonons can be introduced for example by adding stochasticity in the dynamics and we studied this case numerically. We find that in this case the oscillations are qualitatively different from the purely harmonic case and do not survive in the limit of large system size.

ACKNOWLEDGMENTS

APPENDIX: DETAILS OF CALCULATION

Here we give more details of the derivation for the temperature profile and the current. We basically need to evaluate the integral

$$I_i = \frac{m_i \gamma_L}{\pi} \int_{-\infty}^{\infty} d\omega \, \omega^2 |\mathbf{G}_{i1}^+(\omega)|^2, \tag{A1}$$

where $\mathbf{G}^+ = [-\mathbf{M}\omega^2 + \mathbf{\Phi} - \iota\omega\mathbf{\Gamma}]^{-1}$. We consider the case with $k = 1$. Let us define $\Delta_{l,m}$ as the determinant of the submatrix of $[-\mathbf{M}\omega^2 + \mathbf{\Phi} - i\omega\mathbf{\Gamma}]$ that starts from the lth row and column and ends in the mth row and column. We also define $D_{l,m}$ as the determinant of the submatrix of $[-M\Omega^2 + \Phi]$ starting from the lth row and column and ending in the mth row and column. In terms of these one has

$$\mathbf{G}_{l,1}^+(\Omega) = \frac{\Delta_{l+1,N}}{\Delta_{1,N}}, \quad \mathbf{G}_{l,N}^+(\omega) = \frac{\Delta_{1,l-1}}{\Delta_{1,N}}, \tag{A2}$$

with

$$\begin{aligned}
\Delta_{1,l-1} &= D_{1,l-1} - i\omega\gamma_L D_{2,l-1}, \\
\Delta_{l+1,N} &= D_{l+1,N} - i\omega\gamma_R D_{l+1,N-1}, \\
\Delta_{1,N} &= D_{1,N} - \iota\omega(\gamma_R D_{1,N-1} + \gamma_L D_{2,N}) \\
&\quad - \omega^2 \gamma_L \gamma_R D_{2,N-1}.
\end{aligned} \tag{A3}$$

Let us now define $f(l) = D_{1,2l}$ and $g(l) = D_{1,2l-1}$. These satisfy the recursion relation,

$$\begin{bmatrix} f(l) \\ g(l) \end{bmatrix} = \mathbf{B} \begin{bmatrix} f(l-1) \\ g(l-1) \end{bmatrix},$$

where

$$\mathbf{B} = \begin{bmatrix} (2 - m_a\omega^2)(2 - m_b\omega^2) - 1 & -(2 - m_b\omega^2) \\ (2 - m_a\omega^2) & -1 \end{bmatrix},$$
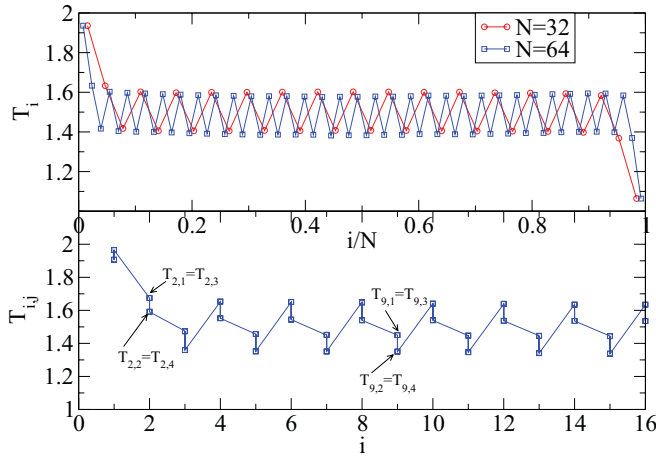

FIG. 8. (Color online) Simulation results for temperature profile for a two-dimensional $N \times W$ strip of harmonically coupled particles with a periodic arrangement of masses. The sites on the strip are labeled (i,j) with $i = 1, \ldots, N$ and $j = 1, \ldots, W$. Particles at sites with even $i + j$ have mass m_a and others have masses m_b. Heat baths are attached to all sites on the layers $i = 1$ (temperature T_L) and $i = N$ (temperature T_R). Periodic boundary conditions are imposed in the transverse (j) direction. Upper plot shows the average temperature on successive layers for chains of lengths $N = 32$ and $N = 64$. There are oscillations in the transverse direction also and this is shown in the lower plot which shows the temperatures $T_{i,j}$ on all sites of a section of the $N = 64$ chain. Note that from symmetry we have $T_{i,j} = T_{i,j+2}$, and this can be observed here. The width of the strips was taken to be $W = 4$. The other parameters were taken to be $m_a = 0.6$, $m_b = 1.4$, $\gamma_L = \gamma_R = 1.0$ and $T_L = 2.0, T_R = 1.0$.

with the initial condition $f(0) = 1$ and $g(0) = 0$. Hence we get

$$\begin{bmatrix} f(l) \\ g(l) \end{bmatrix} = \mathbf{B}^l \begin{bmatrix} 1 \\ 0 \end{bmatrix}. \qquad (A4)$$

The matrix $\mathbf{B}$ has unit determinant and can be expressed in terms of the Pauli spin matrices $\vec{\sigma}$ as follows:

$$\mathbf{B} = \cos q \mathbf{1} + \iota \vec{\sigma} \cdot \vec{n} \sin q = e^{\iota \vec{\sigma} \cdot \vec{n} q},$$

where

$$\cos q = \mathrm{Tr} \frac{\mathbf{B}}{2} = \frac{(2 - m_a \omega^2)(2 - m_b \omega^2) - 2}{2}, \qquad (A5)$$

and $\vec{n}$ is a three-dimensional unit vector. Hence we get

$$\mathbf{B}^l = = e^{\iota \vec{\sigma} \cdot \vec{n} l q} = \cos(lq)\mathbf{1} + \sin(lq)\frac{\mathbf{B} - \cos q \mathbf{1}}{\sin q}. \quad (A6)$$

Combining Eq. (A6) and Eq. (A4) we have

$$f(l) = \frac{\sin(l + 1/2)q}{\sin(q/2)}, \qquad (A7)$$

$$g(l) = \frac{\sin(lq)}{\sin q}(2 - m_a \omega^2). \qquad (A8)$$

Note that for odd-dimensional matrices with the first mass equal to m_b, the determinant would be given by Eq. (A8) with m_a replaced by m_b. Using these expressions in Eqs. (A2) and (A3), we then get the following forms for the integrals I_i, depending on whether N is even or odd.

Case (1) Even N:

$$I_{\mathrm{odd}\, i} = \frac{2m_a \gamma_L}{\pi} \int_0^\infty d\omega \omega^2 \frac{\frac{\sin^2[(N-i+1)q/2]}{\sin^2 q}(2 - m_b \omega^2)^2 + \gamma_R^2 \omega^2 \frac{\sin^2[(N-i)q/2]}{\sin^2(q/2)}}{|\Delta_{1,N}|^2},$$

$$I_{\mathrm{even}\, i} = \frac{2m_l \gamma_L}{\pi} \int_0^\infty d\omega \omega^2 \frac{\frac{\sin^2[(N-i+1)q/2]}{\sin^2(q/2)} + \gamma_R^2 \omega^2 \frac{\sin^2[(N-i)q/2]}{\sin^2 q}(2 - m_a \omega^2)^2}{|\Delta_{1,N}|^2}, \quad I_N = \frac{2\gamma_L m_a}{\pi} \int_0^\infty d\omega \frac{\omega^2}{|\Delta_{1,N}|^2}, \qquad (A9)$$

where

$$\Delta_{1,N} = \left[\frac{\sin \frac{(N+1)q}{2}}{\sin(q/2)} - \gamma_L \gamma_R \omega^2 \frac{\sin \frac{(N-1)q}{2}}{\sin(q/2)} \right] + \iota \omega \left[\gamma_L(2 - m_b \omega^2) + \gamma_R(2 - m_a \omega^2) \right] \frac{\sin(Nq/2)}{\sin q}.$$

Case (2) Odd N:

$$I_{\mathrm{odd}\, i} = \frac{2m_a \gamma_L}{\pi} \int_0^\infty d\omega \omega^2 \frac{\frac{\sin^2[(N-i+1)q/2]}{\sin^2(q/2)} + \gamma_R^2 \omega^2 (2 - m_b \omega^2)^2 \frac{\sin^2[(N-i)q/2]}{\sin^2(q)}}{|\Delta_{1,N}|^2},$$

$$I_{\mathrm{even}\, i} = \frac{2m_l \gamma_L}{\pi} \int_0^\infty d\omega \omega^2 \frac{(2 - m_a \omega^2)^2 \frac{\sin^2[(N-i+1)q/2]}{\sin^2 q} + \gamma_R^2 \omega^2 \frac{\sin^2[(N-i)q/2]}{\sin^2(q/2)}}{|\Delta_{1,N}|^2}, \quad I_N = \frac{2\gamma_L m_a}{\pi} \int_0^\infty d\omega \frac{\omega^2}{|\Delta_{1,N}|^2}, \qquad (A10)$$

where

$$\Delta_{1,N} = \left[(2 - m_a \omega^2) \frac{\sin \frac{(N+1)q}{2}}{\sin q} - \gamma_L \gamma_R \omega^2 (2 - m_b \omega^2) \frac{\sin \frac{(N-1)q}{2}}{\sin q} \right] + \iota \omega (\gamma_L + \gamma_R) \frac{\sin(Nq/2)}{\sin q}.$$

We now consider points in the bulk such that $x = i/N$ and $(N - i)/N$ remain finite in the $N \to \infty$ limit. We now note that, for real values of $0 < q < \pi$, Eq. (A5) has two allowed solutions for ω, namely:

$$\omega_-^2 = \frac{1}{m_a m_b}[1 - \phi(q)],$$

$$\omega_+^2 = \frac{1}{m_a m_b}[1 + \phi(q)],$$

where

$$\phi(q) = [1 - 2m_a m_b(1 - \cos q)]^{1/2}, \quad 0 \leqslant q \leqslant \pi.$$

These correspond to the frequencies in the acoustic and optical branches of the lattice with the frequency ranges $0 < \omega_- < \sqrt{2/M}$ and $\sqrt{2/m} < \omega_+ < \sqrt{2/(mM)}$, where m

(M) is the smaller (larger) of the two masses. For frequencies outside these ranges, Eq. (A5) gives imaginary values of q. This means that for these frequencies, terms such as $\sin Nxq$ grow exponentially with N. Hence it is clear that in the limit $N \to \infty$, the integrals in Eqs. (A9) and (A10) only get contributions from frequencies in the acoustic and optical bands. Thus for each of the integrals above, we get

$$\int_0^\infty d\omega F(\omega) = \int_0^{\sqrt{2/M}} d\omega_- F(\omega_-) + \int_{\sqrt{2/m}}^{\sqrt{2/(mM)}} d\omega_+ F(\omega_+)$$

$$= \int_0^\pi dq \left| \frac{d\omega_-}{dq} \right| - F(\omega_-(q))$$

$$+ \int_0^\pi dq \left| \frac{d\omega_+}{dq} \right| F(\omega_+(q)).$$

We now note from Eqs. (A9) and (A10) that the required integrands $F(\omega)$ have factors of the form $\sin^2(Nxq)$ in the numerators and $\Delta_{1,N}$ in the denominators. In the limit $N \to \infty$ the factors $\sin^2(Nxq)$ in the numerators can be replaced by $1/2$. Next we note that the determinant $\Delta_{1,N}$ always has the form

$$\Delta_{1,N} = A(q)\sin(Nq) + B(q)\cos(Nq), \qquad (A11)$$

where A and B are smooth complex-valued functions. We now obtain the following result for any function $g(\theta,\phi)$ which is periodic in both variables:

$$\lim_{N} \to \infty \int_0^\pi d\theta\, g(\theta, N\theta) = \lim_{N \to \infty} \frac{1}{N} \int_0^{2\pi(N/2)} d\phi\, g\left(\frac{\phi}{N}, \phi\right)$$

$$= \lim_{N \to \infty} \frac{1}{N} \sum_{i=1}^{i=(N/2)} \int_{2\pi(i-1)}^{2\pi i} d\phi\, g\left(\frac{\phi}{N}, \phi\right) = \lim_{N \to \infty} \frac{1}{N} \sum_{i=1}^{i=(N/2)} \int_0^{2\pi} d\psi\, g\left(\frac{2\pi(i-1)+\psi}{N}, \psi\right)$$

$$= \lim_{N \to \infty} \sum_{i=1}^{i=(N/2)} \frac{1}{N} \int_0^{2\pi} d\psi\, g\left(\frac{2\pi(i-1)}{N}, \psi\right) = \frac{1}{2\pi} \int_0^\pi d\theta \int_0^{2\pi} d\psi\, g(\theta, \psi).$$

Using this we obtain

$$\int_0^\pi dq\, \frac{C(q)}{|A(q)\sin(Nq) + B(q)\cos(Nq)|^2} = \int_0^\pi C(q)\, dq\, \frac{1}{2\pi} \int_0^{2\pi} d\psi\, \frac{1}{|A(q)\sin\psi + B(q)\cos\psi|^2}$$

$$= \int_0^\pi dq\, \frac{C(q)}{|A(q)B^*(q) - A^*(q)B(q)|}. \qquad (A12)$$

Using this we get the asymptotic forms of the various integrals in Eqs. (A9) and (A10), and these lead to the results given in Eqs. (11) and (12). When $\gamma_L = \gamma_R = \gamma$, we can explicitly carry out the integrals appearing in these expressions and we get the following results.

Case (1) Even N:

$$I_{\text{odd}} = \frac{m_b}{2} \frac{2(1+\beta) + (\delta^2 + 2\delta)2\beta + 2\frac{\beta^2}{1+2\beta\mu}\delta^2(\delta+1)^2}{\sqrt{2\beta+1}\sqrt{1+2\beta+2\beta^2\mu}} - 4\frac{m_a}{1+2\beta\mu}\left(\sqrt{\frac{1+2\beta+2\beta^2\mu}{1+2\beta}} - 1\right)$$

$$+ \frac{m_b}{2} \frac{|\delta|(\delta+1)^2}{\mu(1+2\beta\mu)\sqrt{1+\delta^2}} + m_a \frac{2\beta\mu}{1+2\beta\mu}\left(1 - \frac{|\delta|}{\sqrt{1+\delta^2}}\right), \qquad (A13)$$

$$I_{\text{even}} = m_a\left(1 + \frac{-(1+\beta) + \beta(2\delta - \delta^2) - \delta^2(1-\delta)^2\frac{\beta^2}{1+2\beta\mu}}{\sqrt{1+2\beta}\sqrt{1+2\beta+2\beta^2\mu}} + \beta\frac{|\delta|(1-\delta)^2}{\sqrt{1+\delta^2}(1+2\beta\mu)}\right)$$

$$+ \frac{m_b}{1+2\beta\mu}\left(-\frac{|\delta|}{\sqrt{1+\delta^2}} + \frac{\sqrt{1+2\beta+2\beta^2\mu}}{\sqrt{1+2\beta}}\right), \qquad (A14)$$

$$J^E = \Delta T \frac{\gamma}{\beta^2\mu(1+4\gamma^2)}[2\beta + 1 + 2\beta^2\mu(1+\delta^2 - |\delta|\sqrt{1+\delta^2}) - \sqrt{(2\beta+1)(2\beta+1+2\beta^2\mu)}], \qquad (A15)$$

where $\mu = 2m_a m_b$, $\delta = m_a - m_b$, $\beta = \gamma^2/(m_a m_b)$.

Case (2) Odd N:

$$I_{\text{odd}} = I_{\text{even}} = \tfrac{1}{2}, \qquad (A16)$$

$$J^O = \Delta T \frac{\gamma B}{G^2}\left(1 - \frac{\sqrt{(F+H)^2 - G^2} + \sqrt{(F-H)^2 - G^2}}{2F}\right), \qquad (A17)$$

where

$$F = \frac{B}{2C}(B^2 - 4AC)^{1/2}, \quad G = C\mu, \quad H = \frac{B^2}{2C} - C(1-\mu) - A$$

and

$$A = \frac{\delta}{m_b} - \frac{\delta\beta}{m_a}, \quad B = \frac{1}{m_b} + \frac{2m_b\beta}{m_a}, \quad C = \frac{\beta}{m_a}.$$

[1] A. Dhar, Adv. Phys. **57**, 457 (2008).

[2] F. Bonetto, J. L. Lebowitz, and L. Rey-Bellet, in *Mathematical Physics 2000*, edited by A. S. Fokas *et al.* (Imperial College Press, London, 2000), p. 128.

[3] S. Lepri, R. Livi, and A. Politi, Phys. Rep. **377**, 1 (2003).

[4] Z. Rieder, J. L. Lebowitz, and E. Lieb, J. Math. Phys. **8**, 1073 (1967).

[5] H. Nakazawa, Suppl. Prog. Theor. Phys. **45**, 231 (1970).

[6] A. Casher and J. L. Lebowitz, J. Math. Phys. **12**, 1701 (1971).

[7] A. J. O'Connor and J. L. Lebowitz, J. Math. Phys. **15**, 692 (1974).

[8] G. Casati, Found. Phys. **16**, 51 (1986).

[9] T. Hatano, Phys. Rev. E **59**, R1 (1999).

[10] A. Dhar, Phys. Rev. Lett. **86**, 3554 (2001).

[11] P. Grassberger, W. Nadler, and L. Yang, Phys. Rev. Lett. **89**, 180601 (2002).

[12] B. Li, G. Casati, J. Wang, and T. Prosen, Phys. Rev. Lett. **92**, 254301 (2004).

[13] A. F. Neto, H. C. F. Lemos, and E. Pereira, Phys. Rev. E **76**, 031116 (2007).

[14] E. Pereira, L. M. Santana, and R. Avila, Phys. Rev. E **84**, 011116 (2011).

[15] P. L. Garrido, P. I. Hurtado, and B. Nadrowski, Phys. Rev. Lett. **86**, 5486 (2001).

[16] T. Mai, A. Dhar, and O. Narayan, Phys. Rev. Lett. **98**, 184301 (2007).

[17] A. Dhar and D. Roy, J. Stat. Phys. **125**, 801 (2006).

[18] H. Risken, *The Fokker Planck Equation* (Springer, Berlin, 1989).

[19] C. Bernardin, J. Stat. Phys. **133**, 417 (2008).

[20] G. Basile, C. Bernardin, and S. Olla, Commun. Math. Phys. **287**, 67 (2009).

[21] A. Dhar, K. Venkateshan, J. L. Lebowitz, Phys. Rev. E **83**, 021108 (2011).

[22] F. Bonetto, J. L. Lebowitz, and J. Lukkarinen, J. Stat. Phys. **116**, 783 (2004).